Separation and Purification Technology 172 (2017) 374–381

Contents lists available at ScienceDirect

Separation and Purification Technology

journal homepage: www.elsevier.com/locate/seppur

Highly photocatalytic activities of magnetically separable reduced graphene oxide-$CoFe_2O_4$ hybrid nanostructures in dye photodegradation

H.-Y. He *, J. Lu

College of Material Science and Engineering, Shaanxi University of Science and Technology, Xi'an, Shaanxi 710021, China

ARTICLE INFO

Article history:
Received 28 September 2015
Received in revised form 25 August 2016
Accepted 31 August 2016
Available online 1 September 2016

Keywords:
Graphene
Hybrids
Heterojuction
Photocatalysis
Fenton-like reaction
Magnetic separation

ABSTRACT

The $CoFe_2O_4$ nanoparticles and reduced graphene oxide-$CoFe_2O_4$ (rGO-$CoFe_2O_4$) hybrid nanostructures with rGO/$CoFe_2O_4$ ratio of 0.05, and 0.1 were hydrothermally synthesized. The microstrutrual and photocatalytic activities of nanoparticles and hybrids were studied in the photodegradation of malachite green in the water. The $CoFe_2O_4$ nanoparticles and them in the hybrids showed uniform granular morphology with average particle sizes of ~17 nm. Because higher valence band energy of the $CoFe_2O_4$, the photogenerated electrons can be transformed from the $CoFe_2O_4$ to the rGO. Therefore, the hybrids showed obviously greater sunlight-excited photocatalytic and Fenton-like photocatalytic activities to the dye degradation, increased as increasing rGO/$CoFe_2O_4$ ratio, than the nanoparticles and increased as increasing rGO/$CoFe_2O_4$ ratio. Moreover, the photodegradation rate is larger at higher initial solution pH = 7 than at pH = 5, whereas the photo-Fenton-like reaction is intenser at higher H_2O_2 concentration. The quasi-kinetic rate constants of the photocatalysis systems are in the range of ~0.43–0.85 h^{-1} and remarkably increase to ~9.21–18.42 h^{-1} by synthetically using H_2O_2. The nanoparticles and hybrids also showed strong ferromagnetic property with the saturation magnetization of ~61.82–63.73 emu/g, which provides a well magnetic separation performance of the nanoparticles and hybrids from the degraded solution.

1. Introduction

Because the graphene possesses the ability to accept the electrons from semiconductor and so prevent recombination of photogenerated electrons and holes, anchoring well-structured photocatalysts onto graphene-based materials can result in the exploration of novel composites with advanced photocatalytic performances. Therefore, the introduction of graphene-related materials (graphene, graphene oxide, and reduced graphene oxide) as catalyst supports into the various photocatalyst system has attracted great interest [1–3], for the reason that the obtained hybrid products were found to display outstanding photocatalytic performances [4–15].

Cobalt ferrite is magnetic semiconductor material that has some unique characteristics: (i) narrow optical bandgap, (ii) nontoxic and abundant in nature, (iii) low cost, and (iv) their magnetic property can provide magnetic separation performance from the aqueous solution as used as a photocatalyst. Thus, the $CoFe_2O_4$ should be reasonable for structuring the rGO-semiconductor heterojunctions with excellent photocatalytic activity.

In the current work, we report on (i) the hydrothermal synthesis and microstructures of $CoFe_2O_4$ nanoparticles and $CoFe_2O_4$-rGO hybrids; (ii) the effects of the rGO/$CoFe_2O_4$ ratio on the photocatalytic and Fenton-like photocatalytic activities of the synthesized hybrids in photodegradation of malachite green dye in the water in the condition of different initial pH.

2. Experimental

The starting materials used were all analytic grade chemicals without any further processing. Graphene oxide (GO, Jining LeaderNano Tech L.L.C., China) was first ultrasonically dispersed in deionized water to form dispersion solution. Cobalt chloride ($CoCl_2{\cdot}6H_2O$, Shenyang Hua Bai Tai Chemical Co. Ltd, China) and iron nitrate ($Fe(NO_3)_3{\cdot}9H_2O$, Beijing Baishunchem. Co. Ltd., China) were used as starting materials. The chemicals were dissolved in 15 ml deionic water according to the required stoichiometric proportions of $CoFe_2O_4$. For the synthesis of the $CoFe_2O_4$/rGO hybrids, the cobalt chloride and iron nitrate were directly dissolved into the GO aqueous solution. Mass ratio of GO/$CoFe_2O_4$ were designed to be 0.05 and 0.10. The values of the all solutions were expanded to 15 ml with deionic water. The concentration of Fe^{3+} in the such solutions was all 0.2 mol l^{-1}. NaOH with triple gram equivalents of

---

* Corresponding author.
E-mail address: hehy@sust.edu.cn (H.-Y. He).

http://dx.doi.org/10.1016/j.seppur.2016.08.040
1383-5866/

all metal cations was dissolved in small amount of deionic water (~3 ml) and completely dropped into the solutions with magnetic stirring. This relative large amount of NaOH addition can assures the solution pH > 10 throughout and so full precipitation of the all cations. The precursor solutions were then transferred into autoclaves (volume: 25 ml, degree of filling: ~80 vol.%). After sealing, the hydrothermal reaction was then carried out in a oven at 180 °C for 24 h. After natural cooling in the oven, the products were washed repeatedly with distilled water until washing water pH ~ 7, and then dried at 100 °C for 24 h.

The crystalline structural phase of the synthesized nanoparticles and hybrids was identified at room temperature using an X-ray diffractometer (XRD, $CuK_{\alpha1}$, $\lambda = 0.15406$ nm, Model No: D/Max--2200PC, Rigaku, Japan). The morphology of the nanoparticles and hybrids was analyzed using field emission scanning electron microscope (SEM, Model No: S-4800, Hitachi, Japan). The hybrids were adhered on the glass slides with thin transparent adhesive agent, in order that the transmittance, reflectance and absorbance spectra of the nanoparticles and hybrids were determined with an ultraviolet–visible spectrophotometer (Model No: UV2600, SDPTOP, Shanghai, China). The magnetic property was measured with a vibrating sample magnetometer (VSM, Model No: Versa Lab, Quantun Design, USA)

To investigate the photocatalytic activity of the synthesized photocatalysts. The malachite green ($C_{23}H_{25}ClN_2$, Tianjing Basifu chemical L.L.C., China) is used as a substrate and dissolved in deionic water to form aqueous solution with a concentration of 5×10^{-6} M. One group of the solution were additionally adjusted to initial pH = 5 with diluted HCl aqueous solution. In each experiment, 50 ml malachite green aqueous solution and 50 mg synthesized photocatalysts were added into a glass beaker. In two other groups of the solutions with pH = 7, 0.5 ml and 1.0 ml hydrogen peroxide (H_2O_2) were added, respectively. The photocatalysis experiment was carried out under the sunlight with average intensities of ~350 W/m^2. After each irradiation times of 0, 30, 60, 90, and 120 min, ~3 ml solutions were taken out and subsequently measured for their absorbances on a spectrophotometer (Model No: 722 N, Hengping, China). The solutions after the test were returned to the beakers to maintain the normal volume of the solutions under test.

In first hour of the above process, the oxidation-reduction potentials (ORP) of the malachite green aqueous solutions in all photocatalysis conditions were measured with an oxidation-reduction potential tester (Model no: ORP-286, China). The ORP of the nanoparticles and hybrids surfaces were evaluated by the differences of the oxidation-reduction potentials of the malachite green aqueous solutions with and without the photocatalysts.

The quasi-kinetic rate constant (k_1) was calculated with the kinetic relation between the concentration (C) of the malachite green in the water and the photocatalytic reaction time (t) given by:

$$\frac{C}{C_0} = A\exp\left(-\frac{k_1 t}{T}\right) \tag{1}$$

In which, C_0 is the initial concentration, T is reaction temperature, and A is a constant.

3. Results and discussion

3.1. XRD analysis

Fig. 1a shows the XRD patterns of the synthesized nanoparticles and hybrids. All diffraction peaks match with the reported powder diffraction data of hexogoanl $CoFe_2O_4$ (JCPDS: 22-1086). This indicates that the nanohybrids are single phase $CoFe_2O_4$ without any other impurities. Crystallites size (D) was estimated from the full width (in radian) at half maximum (β) of the diffraction peak at $2\theta \sim 35.5°$ according to the Scherrer's equation:

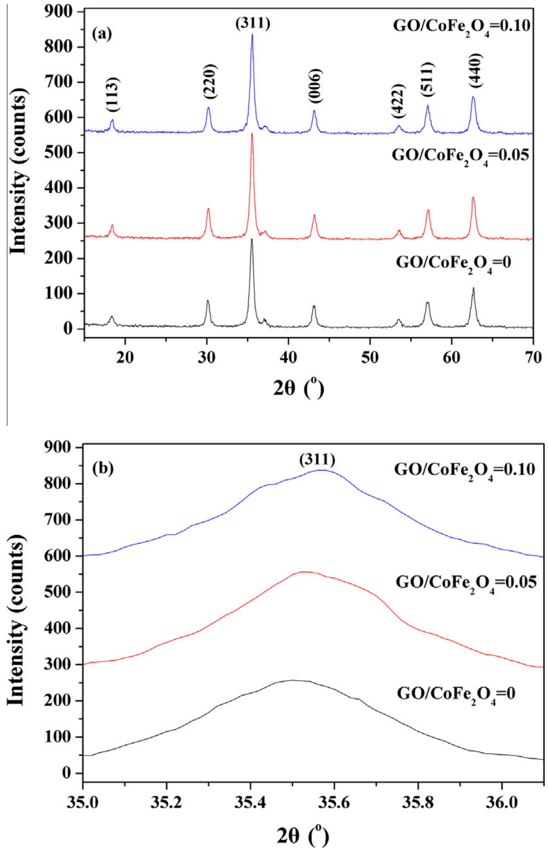

Fig. 1. (a) XRD patterns and (b) strongest (311) XRD peak patterns of the $CoFe_2O_4$ particles and hybrids.

$$D = 0.9\frac{\lambda}{\beta\cos\theta} \tag{2}$$

where λ is the X-ray wavelength. Estimated sizes are ~16.9 nm, ~17.3 nm, and ~17.5 nm for the nanoparticles and hybrids with the $rGO/CoFe_2O_4$ of 0.025and 0.05, respectively. The strongest (311) peak shifts from ~35.50° to higher ~24.53° and ~35.57° as increasing $rGO/CoFe_2O_4$ ratio form 0 to 0.05 and 0.1 (Fig. 1b). This indicates a lattice shrink on basis of Bragg's equation. The increase in the average particle size and lattice shrink could imply that the rGO favors the growth and crystallization of the $CoFe_2O_4$ crystallites.

3.2. SEM analysis

Fig. 2 shows typical SEM micrographs of the nanoparticles and hybrids. The $CoFe_2O_4$ nanoparticles show granular particle morphology. As the graphene oxide are introduced, the nanoparticles show similar particle morphology. But the partial nanoparticles are completely adhered on the reduced graphene oxide, forming large platelike morphology. The nanoparticles in three samples have average particle size of ~18 nm, close to the result determined by XRD analysis.

3.3. Raman and FTIR spectra analyses

Raman spectroscopy, a nondestructive method, is also a useful technique to explore the crystalline or molecular changes after